Dalton Transactions

Accepted Manuscript

ROYAL SOCIETY OF CHEMISTRY

www.rsc.org/dalton

POM Species, Temperature and Counterions Modulated the Various Dimensionalities of POM-based Metal-Organic Frameworks

Jing-Wen Sun,[†] Peng-Fei Yan,[*,†] Guang-Hui An,[†] Jing-Quan Sha,[‡] Cheng Wang,[†] and Guang-Ming Li[*,†]

[†]*Key Laboratory of Functional Inorganic Material Chemistry (MOE), P. R. China; School of Chemistry and Materials Science, Heilongjiang University; Harbin, 150080, P. R. China;* [‡]*School of Pharmacy, Jiamusi University, Jiamusi, 154007, P. R. China*

ABSTRACT:

To investigate the influence of POM species, temperature and counterions on the structures of POM–MOFs containing Cu-tda second building blocks (SBUs), six new complexes with various dimensionalities, e. g. three dimension (3D) $[Cu(H_2tda)(H_2O)_2]_4[SiW_{12}O_{40}]\cdot 12H_2O$ (**1**), two dimension (2D) $[Cu_2(H_2tda)_2(H_2O)_3]\cdot[Cu(H_2tda)(H_2O)_2]\cdot[PMo_{12}O_{40}]\cdot 5H_2O$ (**2**), H-bond 2D $[Cu(H_2tda)(H_2O)_2]_3\cdot[PMo_{12}O_{40}]\cdot[Cu(Htda)(H_2O)_3]\cdot 8H_2O$ (**3**), one dimension (1D) $[Cu_2(H_2tda)_2(H_2O)_4]_2\cdot[Cu_2(tda)_2(H_2O)_4]\cdot[HPW_{12}O_{40}]\cdot 5H_2O$ (**4**), 1D $[Cu_2(H_2tda)_2(H_2O)_4][SiW_{12}O_{40}]\cdot(TMA)_2\cdot 3H_2O$ (**5**), and zero dimension (0D) $[Cu(H_2tda)(H_2O)_3][SiW_{12}O_{40}]\cdot(TMA)_3\cdot H_2O$ (**6**), were isolated depending on the reaction conditions. It is observed that the POM species, temperature and counterions exhibit essential effect on the structures, which results in the formation of various dimensional POM-MOF complexes **1–6**. In addition, photocatalytic degradation of RhB by complexes **1**, **5** and **6** under UV irradiation were also investigated.

INTRODUCTION

Metal–organic frameworks (MOFs) built from transition metal ions and organic bridging ligands have evoked increasing interest in recent years not only from their promising applications but also from their intriguing aesthetic appeal and topologies.[1-8] Polyoxometalates (POMs), an outstanding class of inorganic building blocks with abundant topologies and great potential applications in catalysis,[9-13] magnetism,[14] and materials science,[15-17] are widely used to link variable transition-metal complexes (TMC)s for the construction of various hybrid complexes, so-called POM-based metal–organic frameworks (POM-MOFs).[18-23] The POM-MOFs combining the advantages of both POMs and MOFs may open up new possibilities in the pursuit of multifuncational materials with designed functional properties and aesthetic topological structures. Since the final structures are frequently modulated by various factors, such as solvent systems, pH value, counterions, temperature,

and steric hindrance, length, and flexibility of organic ligands,[24-33] the dimensionality control of the POM-MOFs complexes is still a great challenge from the crystal engineering point of view although many novel POM-MOFs have been successfully synthesized.[34] In our previous work, we have discussed the influence of steric hindrance of organic ligands, and secondary spacers on the dimension of POM-MOFs.[35] To further investigate the effect of the reaction temperature and counterions on the dimensioinality control of POM-MOFs, we choose 1,2,3-triazole-4,5-dicarboxylic acid (H_3tda) as linking ligand for the design of initial high dimensional POM-MOFs owing to its small steric hindrance and ability to chelate multiple metal sites. Although H_3tda ligand have been proved to be very interesting and useful in various applications, particularly in the extended 2D and 3D MOF family, the introduction of H_3tda ligands in POMs is less explored.[36] Therefore, H_3tda was employed in the reactions of Cu(II) ions and Keggin POMs to assemble POM-MOFs in this paper. First of all, a three-dimensional (3D) complex **1** was isolated. Upon changing POMs species, reaction temperature, and introduction of counterions TMAH (TMAH = tetramethylammonium hydroxide) into the reaction system of **1**, complexes **2–6** with various structures, including the 0D, 1D and 2D frameworks, are obtained. More specifically, these are 3D $[Cu(H_2tda)(H_2O)_2]_4\cdot[SiW_{12}O_{40}]\cdot 9H_2O$ (**1**), 2D $[Cu_2(H_2tda)_2(H_2O)_3]\cdot[Cu(H_2tda)(H_2O)_2]\cdot[PMo_{12}O_{40}]\cdot 5H_2O$ (**2**), H-bond 2D $[Cu(H_2tda)(H_2O)_2]_3\cdot[PMo_{12}O_{40}]\cdot[Cu(Htda)(H_2O)_3]\cdot 8H_2O$ (**3**), 1D $[Cu_2(H_2tda)_2(H_2O)_4]_2\cdot[Cu_2(tda)_2(H_2O)_4]\cdot[HPW_{12}O_{40}]\cdot 18H_2O$ (**4**), 1D $[Cu_2(H_2tda)_2(H_2O)_4]\cdot[SiW_{12}O_{40}]\cdot(TMA)_2\cdot 3H_2O$ (**5**), and 0D $[Cu(H_2tda)(H_2O)_3]\cdot[SiW_{12}O_{40}]\cdot(TMA)_3\cdot H_2O$ (**6**). The roles of the POM clusters, temperature and counterions on the structural modulation of the POM-MOFs complexes have been discussed in this paper. Therefore, the photocatalytic properties of complexes **1**, **5** and **6** were investigated in detail.

EXPERIMENTAL SECTION

Materials and Methods All chemicals were obtained from commercial sources and used without further purification. Elemental (C, H and N) analyses were performed on a Perkin-Elmer 2400 analyzer. FT-IR data were collected on a Perkin-Elmer 100 spectrophotometer by using KBr pellets in the range of 450−4500 cm^{-1}. UV spectra (in methanol) were recorded on a Perkin-Elmer 35 spectrophotometer. Thermal analyses were carried out on a STA-6000 with a heating rate of 10 °C min^{-1} in a temperature range from 30 °C to 800 °C in atmosphere. Powder X-ray diffraction (PXRD) data were recorded on a Rigaku D/Max-3B X-ray diffractometer with CuKα as the radiation source (λ = 0.15406 nm) in the angular range θ = 5−50º at room temperature.

Synthesis of $[Cu(H_2tda)(H_2O)_2]_4\cdot[SiW_{12}O_{40}]\cdot 9H_2O$ (1). $CuCl_2\cdot 2H_2O$ (150 mg, 0.88 mmol), H_3tda (30 mg, 0.19 mmol) and $H_4SiW_{12}O_{40}$ (300 mg, 0.10 mmol) were dissolved in 24 mL distilled water, which was heated at 100 ^oC for 2 h. The filtered was kept at room temperature for slow evaporation. Blue crystals of **1** were isolated over the course of one month (yield: ~71% based on W). IR (KBr, cm^{-1}) for complex **1**: 1667(s), 1600(s), 1471(s), 1341(w), 1299(w), 1277(w), 1241(w), 1125(m), 1015(m), 971(s), 923(s), 886(s), 803(s); Elemental Anal. Calcd (Found %) for $C_{16}H_{42}N_{12}Cu_4SiW_{12}O_{73}$ (4058.89): C, 4.73 (4.74); H, 1.04 (1.03); N, 4.14 (4.13).

Synthesis of $[Cu_2(H_2tda)_2(H_2O)_3]\cdot[Cu(H_2tda)(H_2O)_2]\cdot[PMo_{12}O_{40}]\cdot 5H_2O$ (2). Complex **2** was synthesized following the same procedure as that of **1** using $H_3PMo_{12}O_{40}$ (300 mg, 0.16 mmol) in the place of $H_4SiW_{12}O_{40}$.Green crystals of **2** were isolated over the course of one month (yield: ~72% based on Mo). IR (KBr, cm^{-1}) for complex **2**: 1648(s), 1595(m), 1472(m), 1298(w), 1249(w), 1142(w), 1061(s), 962(s), 882(m), 808(s), 697(m); Elemental Anal. Calcd (Found %) for $C_{12}H_{26}N_9Cu_3PMo_{12}O_{62}$ (2661.25): C, 5.42 (5.45); H, 0.98 (0.96); N, 4.74 (4.73).

Synthesis of $[Cu(H_2tda)(H_2O)_2]_3\cdot[PMo_{12}O_{40}]\cdot[Cu(Htda)(H_2O)_3]\cdot 8H_2O$ (3). Complex **3** was synthesized following the same procedure as that of **2** except that stir at room temperature. Green crystals of **3** were isolated over the course of one month (yield: ~74% based on Mo). IR (KBr, cm^{-1}) for complex **3**: 1675(s), 1596(s), 1473(s), 1403(m), 1295(w), 1240(w), 1196(w), 1143(m), 1060(s), 960(s), 869(m), 803(s), 754(s), 704(m); Elemental Anal. Calcd (Found %) for $C_{16}H_{41}N_{12}Cu_4PMo_{12}O_{73}$ (3005.97): C, 6.39 (6.35); H, 1.37 (1.35); N, 5.59 (5.60).

Synthesis of $[Cu_2(H_2tda)_2(H_2O)_4]_2\cdot[Cu_2(tda)_2(H_2O)_4]\cdot[HPW_{12}O_{40}]\cdot 18H_2O$ (4). $CuCl_2\cdot 2H_2O$ (150 mg, 0.88 mmol), H_3tda (30 mg, 0.19 mmol), $H_3PW_{12}O_{40}$ (300 mg, 0.10mmol) and two drop tetramethylammonium hydroxide (TMAH) (25% in water) were dissolved in 24 mL distilled water, which was heated at 100 ^oC for 2 h. The filtered was kept at room temperature for slow evaporation. Blue crystals of **4** were isolated over the course of one month (yield: ~75% based on W). IR (KBr, cm^{-1}) for complex **4**: 1665(s), 1587(s), 1472(s), 1403(m), 1297(w), 1241(w), 1141(w), 1099(m), 1058(s), 955(s), 886(s), 816(s), 748(s), 699(m); Elemental Anal. Calcd (Found %) for $C_{24}H_{60}N_{18}Cu_6PW_{12}O_{94}$ (4723.13): C, 6.10 (6.12); H, 1.28 (1.30); N, 5.34 (5.32).

Synthesis of $[Cu_2(H_2tda)_2(H_2O)_4][SiW_{12}O_{40}]\cdot(TMA)_2\cdot 3H_2O$ (5). Complex **5** was synthesized following the same procedure as that of **4** using $H_4SiW_{12}O_{40}$ (300 mg, 0.10 mmol) in the place of $H_3PW_{12}O_{40}$. Blue crystals of **5** were isolated over the course of one month

(yield: ~73% based on W). IR (KBr, cm^{-1}) for complex **5**: 1667(s), 1600(s), 1482(s), 1417(w), 1297(w), 1252(w), 1141(w), 1015(m), 973(s), 920(s), 884(s), 792(s); Elemental Anal. Calcd (Found %) for $C_{16}H_{42}N_8Cu_2SiW_{12}O_{55}$ (3587.78): C, 5.36 (5.38); H, 1.18 (1.20); N, 3.12 (3.11).

Synthesis of $[Cu(H_2tda)(H_2O)_3][SiW_{12}O_{40}]\cdot(TMA)_3\cdot H_2O$ (6) Complex **6** was synthesized following the same procedure as that of **5** except that stir at 70 ^oC. Blue crystals of **6** were isolated over the course of one month (yield: 71% based on W). IR (KBr, cm^{-1}) for complex **6**: 1650(s), 1594(s), 1472(s), 1411(w), 1298(w), 1248(w), 1141(w), 1062(w), 960(s), 882(s), 807(s), 698(m); Elemental Anal. Calcd (Found %) for $C_{12}H_{34}N_5CuSiW_{12}O_{48}$ (3314.11): C, 4.35 (4.33); H, 1.03 (1.02); N, 2.11 (2.15).

X-ray Crystallographic Analysis. Crystal dates of complexes **1**–**6** were selected on an Oxford Xcalibur Gemini Ultra diffractometer using graphite-monochromated Mo-Kα radiation (λ = 0.71073 Å) at room temperature. Structures of **1–6** were solved using Patterson methods (SHELXS-97), expanded using Fourier methods and refined using SHELXL-97 (full-matrix least-squares on F^2) and WinGX v1.70.01 programs packages.[37] All non-hydrogen atoms were refined anisotropically. Empirical absorption corrections based on equivalent reflections were applied. In complex **1**, the contribution of HIGHLY disordered anions/solvent molecules were treated as diffuse using the Squeeze procedure implemented in the Platon program.[38] The resulting new files were used to further refine the structures. The Squeeze results are consistent with TG and elemental analysis, which indicate that there are nine water molecules as free guests. These water molecules are added in the molecular formula. During the refinement, the command "ISOR" and "DELU" were used to restrain the non-H atoms with ADP and NPD problems, which led to relative high restraint values: 302 for complex **1**, 6 for complex **3**, 6 for complex **4**, 106 for complex **5**, 360 for complex **6**. The command "ISOR" was used to refine atoms O3, O5, O14, O16, O18, O28, O29, O37, O38, O44, O57, O60, O61, O64, N1, N5, N6, N7, N12, C3, C4, C6, C9, C10, C13, and C15 in complex **1**; O15 in complex **4**; N2, O10, O12, O14, O18, and O2W in complex **5**; O15, O42, O65, O75, O78, O82, O97, O105, O3W, O4W, O5W, N1, N2, N4, N5, N6, C5, and C21 in complex **6**. Additionally, restraint command "DELU" was used to average the thermal parameters of atoms with similar environments along the bond for complexes **1**, **5**, and **6**. It refined atoms N7, C13, C15, C16, O37, and O41; C11, C12, N1, O62, and O63; N12, C16, O60, and O61; O41 and O3W in complex **1**; It refined atoms N6, C9, C10, C11, and C12; N4, C5, C6, C7, and C8 in complex **5**; N5, C5, C6, C7, and C8 in complex **6.** The restraint command "SIMU" was used to average the thermal parameters of atoms with same environments for complexes **1**, **5**, and **6**. It refined atoms N7, C13, C15, C16, O37, and O41; C11, C12, N1,

O62, and O63; N12, C16, O60, and O61; O41 and O3W in complex **1**; N4, C5, C6, C7, and C8 in complex **5**; N6, C9, C10, C11, and C12; N5, C5, C6, C7, and C8 in complex **6**. The restraint commands "DFIX" and "DANG" were used to fix the position of atoms for complexes **1**, **3**, and **6**. It refined atoms H131, H140, O3W, H501, H502, and O4W in complex **3**; N6, C9, C10, C11, and C12 in complex **6.** The positions of hydrogen atoms were calculated theoretically. The Keggin PO_4 group in complex **4** and SiO_4 group in complex **5** are disordered by symmetry, which is usual for Keggin structures, and the O7, O12, O13 and O14 atoms in **4** and O5, O6, O7 and O8 atoms in **5** are refined isotropic-parameters as other O atoms with half occupancy. The crystal data and structure refinements of complexes **1**–**6** are summarized in Table 1. The interactions between guests and host frameworks are elaborated in Figure S1–5 and Tables S1–5. Selected bond lengths and angles for complexes **1**–**6** are listed in Tables S6–11. Crystallographic data for the structures reported in this paper have been deposited in the Cambridge Crystallographic Data Center with CCDC Nos. 1425299−1425304 for **1**−**6**.

Table 1 Crystal Data and Structure Refinement for Complexes **1**−**6**

	1	**2**	**3**	**4**	**5**	**6**
Empirical formula	$C_{16}H_{42}N_{12}Cu_4SiW_{12}O_{73}$	$C_{12}H_{26}N_9Cu_3PMo_{12}O_{62}$	$C_{16}H_{41}N_{12}Cu_4PMo_{12}O_{73}$	$C_{24}H_{60}N_{18}Cu_6PW_{12}O_{94}$	$C_{16}H_{42}N_8Cu_2SiW_{12}O_{55}$	$C_{12}H_{34}N_5CuSiW_{12}O_{48}$
Formula weight	4058.89	2661.25	3005.97	4723.13	3587.78	3314.11
Crystal system	Triclinic	Triclinic	Monoclinic	Triclinic	Monoclinic	Monoclinic
space group	$P\bar{1}$	$P\bar{1}$	$P2_1/c$	$P\bar{1}$	$C2/c$	$P2_1/c$
a /Å	13.052(5)	12.635(5)	13.068(5)	14.091(5)	19.474(5)	11.633(5)
b /Å	16.309(5)	12.955(5)	25.151(5)	14.931(5)	14.863(5)	41.370(5)
c /Å	19.758(5)	23.035(5)	25.404(5)	15.928(5)	22.876(5)	15.438(5)
α (deg)	72.567(5)	74.524(5)	90	63.423(5)	90°	90
β (deg)	88.003(5)	74.129(5)	107.650(3)	64.085(5)	106.428(5)	128.24(2)
γ (deg)	81.935(5)	81.539(5)	90	64.562(5)	90	90
V (Å^3)	3973(2)	3482(2)	7957(4)	2579.1(15)	6351(3)	5851(4)
Z	2	2	4	1	4	4
D_c (g·cm^{-3})	3.237	3.116	2.491	2.879	3.740	3.753
T (K)	293(2)	293(2)	293(2)	293(2)	293(2)	293(2)
λ (Mo K$_\alpha$)(Å)	0.71073	0.71073	0.71073	0.71073	0.71073	0.71073
Reflections collected	14004	12272	14017	9085	5612	10315
μ (mm^{-1})	18.461	3.116	3.013	14.655	22.423	23.962
F(000)	3420.0	2502.0	5672.0	2011.0	6328.0	5800.0
Final $R1^a$, $wR2^b$	0.0917,	0.0386,	0.438,	0.0481,	0.0753,	0.1334,
[$I > 2\sigma(I)$]	0.2467	0.0938	0.1082	0.1045	0.0818	0.2566
Final $R1^a$, $wR2^b$	0.1235,	0.0499,	0.589,	0.0555,	0.1479,	0.1614,
(all data)	0.2749	0.1000	0.1189	0.1071	0.1512	0.2738
GOF on F^2	1.041	1.034	1.070	1.180	1.235	1.090

[a] $R_1 = \Sigma^{||}F_0|-|F_c^{||}/\Sigma|F_0|$. [b] $wR_2 = \Sigma[w(F_0^2 - F_c^2)^2]/\Sigma[w(F_0^2)^2]^{1/2}$.

RESULTS AND DISCUSSION

Structural description of $[Cu(H_2tda)(H_2O)_2]_4\cdot[SiW_{12}O_{40}]\cdot 9H_2O$ (1). Single crystal X-ray diffraction study reveals that the structure of **1** is a 3D POM-based MOF constructed from $[Cu(H_2tda)]_2$ second building units (SBUs) and $[SiW_{12}O_{40}]^{4-}$ bricks (abbreviated to SiW_{12}). The unit of complex **1** consists of four Cu(II) ions, four H_2tda ligands and one SiW_{12} cluster (Figure 1a). Each SiW_{12} cluster acts as a tetra-dentate inorganic ligand coordinating with four Cu(II) ions (Figure 1b). In **1**, there are four unique Cu(II) ions, all of them adopt a octahedral geometry coordinated by two nitrogen atoms from two H_2tda ligands, four oxygen atoms from one H_2tda ligands, one SiW_{12} cluster and two water molecules. The most important feature of complex **1** is that it contains an unprecedented 2-fold interpenetration of diamond-like network in POM hybrid material. Such an intriguing structure can be described in detail as follows: first of all, Cu1(II) di-nuclear SBUs and Cu4(II) di-nuclear SBUs link SiW_{12} clusters to form 1D "Z-type" chains (Figure 1c). Furthermore, the adjacent chains are bridged by Cu2(II) SBUs, which leading to 2D layer with large void (~ 10 Å) (Figure 1d). In the vertical direction, the Cu3(II) SBUs connect the neighboring layers result in the 3D structure (Figure 1e). As a result, this 3D structure is a 4-connected diamond-like network in which the 4-connected nodes are SiW_{12} polyoxoanions (Figure 1f). Another feature is that there is POM-SBUs channel in the complex **1** (Figure S6). Interestingly, due to the large pore of the channels and to support the stability of the structure, two identical channels

interpenetrate on another to achieve a two-fold interpenetrated architecture (Figure 1g). To our knowledge, this is the first example of a two-fold interpenetrated feature constructed by a POM-based metal-organic hybrid with ***dia*** topology (Figure 1h).

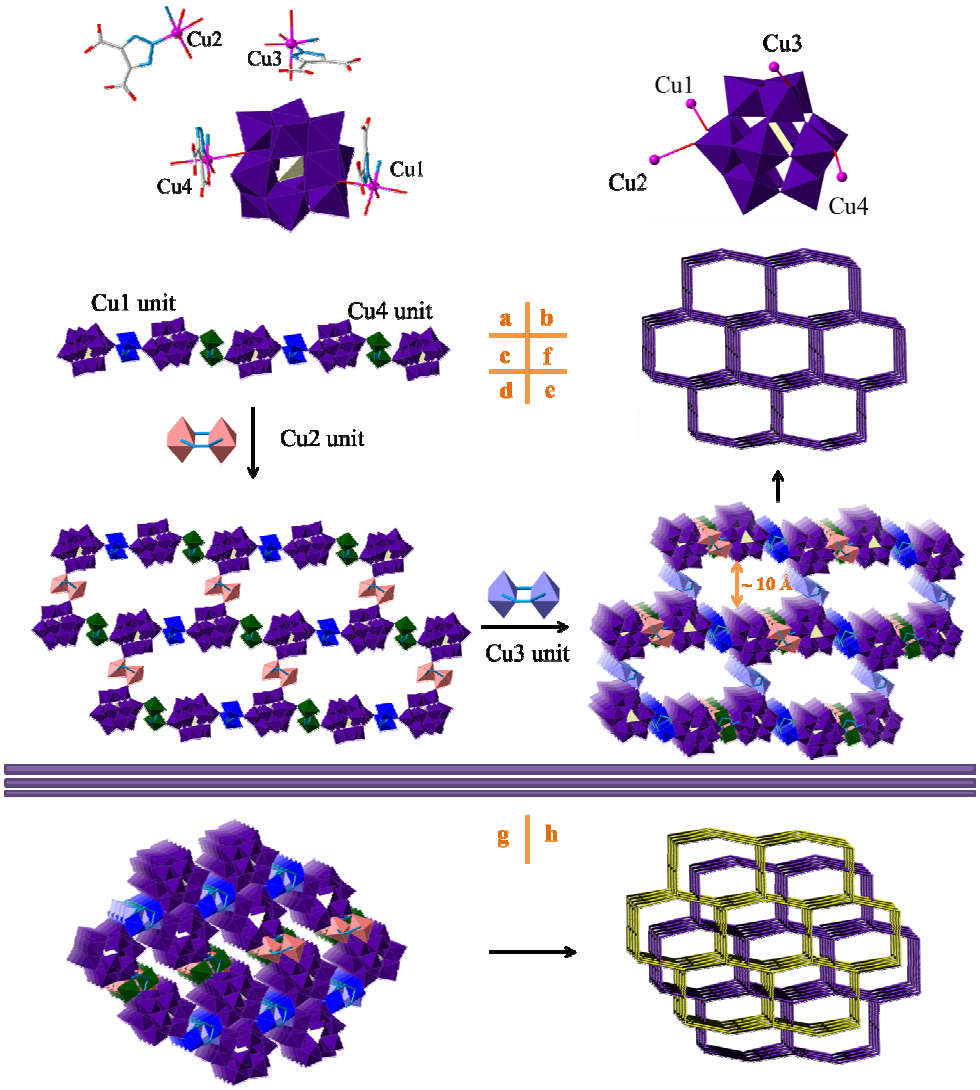

Figure 1. (a) The molecular structure unit of **1**. (b) The coordination view of the SiW_{12} cluster. (c) The 1D chain consisting of Cu1(II) di-nuclear SBUs, Cu4(II) di-nuclear SBUs and SiW_{12} clusters in complex **1**. (d) 1D chains linked by Cu2(II) di-nuclear SBUs into a 2D layer. (e) 2D layers linked by Cu3(II) di-nuclear SBUs into a 3D net. (f) The single ***dia*** topology in complex **1**. (g) Two-fold interpenetrated channels. (h) The two-fold interpenetrated ***dia*** topology in complex **1**. Cu, pink; N, blue; O, red; SiW_{12}, violet; C, gray.

Structural description of $[Cu_2(H_2tda)_2(H_2O)_3]\cdot[Cu(H_2tda)(H_2O)_2]\cdot[PMo_{12}O_{40}]\cdot 5H_2O$ (2). Complex **2** crystallizes in the monoclinic crystal system with the $P2_1/c$ space group. X-ray

structure determination reveals that complex **2** is a 2D layer structure constructed by 1D double chains. The unit comprising three Cu(II) ions, three H_2tda ligands, one $[PMo_{12}O_{40}]^{3-}$ cluster (abbreviated to PMo_{12}) and ten water molecules (Figure 2a). Each PMo_{12} cluster acts as a tri-dentate inorganic ligand coordinating with three Cu(II) ions (Figure 2b). In **2**, there are three unique Cu(II) ions, all of them adopt a octahedral geometry coordinated mode: Cu1(II) centers are coordinated by two nitrogen atoms from two H_2tda ligands, four oxygen atoms from one H_2tda ligands, one PMo_{12} cluster and two water molecules; While Cu2(II) centers are coordinated by two nitrogen atoms from two H_2tda ligands, four oxygen atoms from one H_2tda ligands, one water molecule and two PMo_{12} clusters; Cu3(II) centers are coordinated by two nitrogen atoms from two H_2tda ligands, four oxygen atoms from two H_2tda ligands and two water molecules. Similar to complex **1**, 1D SBUs-POMs chain are obtained in which the di-nuclear SBUs are composed of Cu2(II) and Cu3(II) ions (Figure 2c). Furthermore, the adjacent 1D chains are connected by Cu1(II) SBUs to form a 1D double chains (Figure 2d). If the Cu···O interactions (2.950 Å) were considered as weak interactions, the neighboring 1D double chains will expand to 2D layer (Figure 2e). From a topological point of view, if the PMo_{12} clusters and Cu2(II)-Cu3(II) di-nuclear SBUs are considered as 3-connected nodes, and Cu1(II) SBUs are considered as linear linker. The structure of **2** can be simplified as a ***hcb*** net (Figure 2f).

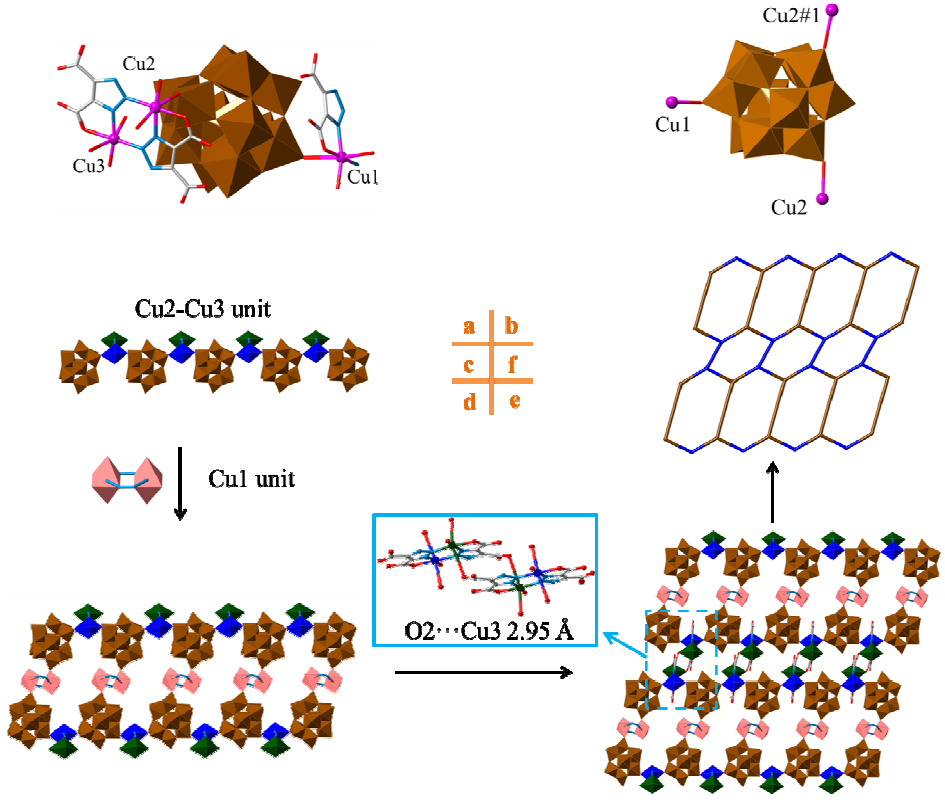

Figure 2. (a) The molecular structure unit of **2**. (b) The coordination view of the PMo_{12} cluster. (c) The 1D chain consisting of Cu2(II)-Cu3(II) di-nuclear SBUs and PMo_{12} clusters in complex **2**. (d) 1D chains linked by Cu1(II) di-nuclear SBUs into a 1D double chain. (e) 1D double chains linked by weak Cu···O interactions into a 2D layer. (f) The topology of the 2D layer. Cu, pink; N, blue; O, red; PMo_{12}, brown; C, gray. (symmetry code: #1: *1+x, y, z*).

Structural description of $[Cu(H_2tda)(H_2O)_2]_3 \cdot [PMo_{12}O_{40}] \cdot [Cu(Htda)(H_2O)_3] \cdot 8H_2O$ (3). Complex **3** crystallizes in the monoclinic crystal system with the $P2_1/c$ space group. X-ray structure determination reveals that complex **3** is a 2D supermolecular layer structure constituted of 1D double chain and di-nuclear Cu(II) spacer. The unit comprising four Cu(II) ions, three H_2tda ligands, one Htda ligand, one $[PMo_{12}O_{40}]^{3-}$ cluster and seventeen water molecules (Figure 3a). Each PMo_{12} cluster acts as a tri-dentate inorganic ligand coordinating with three copper centers (Figure 3b). In **3**, there are four unique Cu(II) ions, all of them adopt a octahedral geometry coordinated mode: Cu1(II), Cu2(II) and Cu4(II) ions are coordinated by two nitrogen atoms from two H_2tda ligands, four oxygen atoms from one H_2tda ligands, one PMo_{12} cluster and two water molecules; While Cu3(II) ions is coordinated by two N atoms from two H_2tda ligands, four O atoms from one H_2tda ligands and three water molecules. Similar to complex **2**, 1D SBUs-POMs chain are connected by Cu4 SBUs to form a 1D double chains (Figure 3c and d). Furthermore, the coordinated water molecules of Cu3 SBUs have an H-bond interactions (the distance is 2.458 Å) to PMo_{12} polyoxoanions, which lead to the final 2D supermolecular layer (Figure 3e). If each PMo_{12} polyoxoanion treat as a 4-connected node, the 2D layer can be simplified as a **sql/Shubnikov** tetragonal plane net with $\{4^4 \cdot 6^2\}$ topology (Figure 3f).

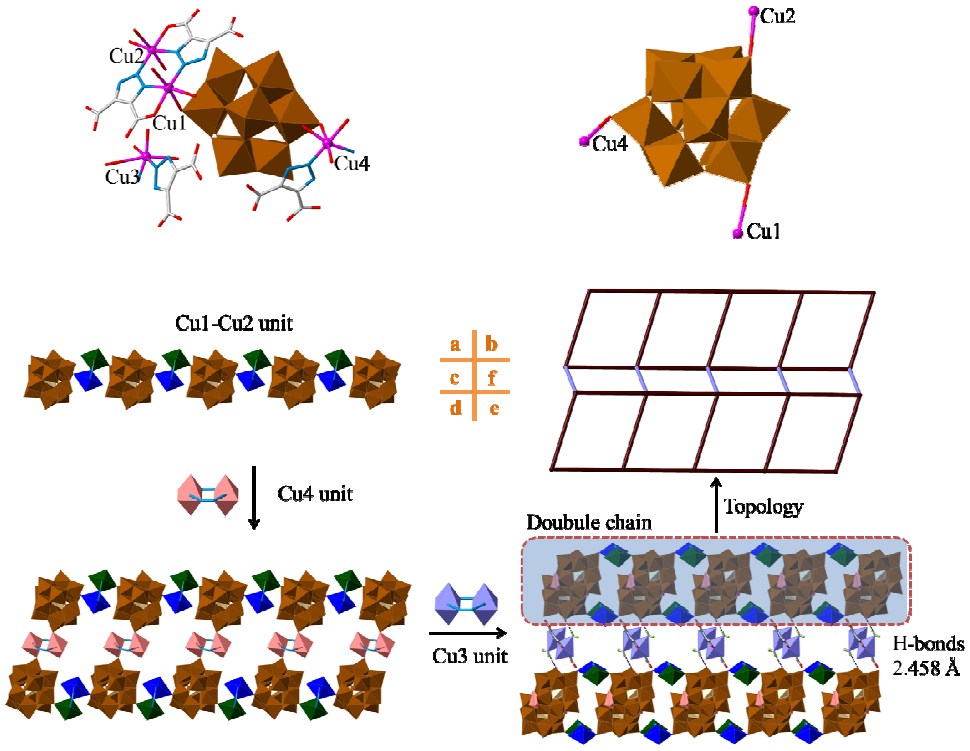

Figure 3. (a) The molecular structure unit of **3** (left). (b) The coordination view of the PMo_{12} cluster. (c) The 1D chain consisting of Cu1(II)-Cu2(II) di-nuclear SBUs and PMo_{12} clusters in complex **3**. (d) 1D chains linked by Cu4(II) di-nuclear SBUs into a 1D double chain. (e) 1D double chains linked by Cu3(II) di-nuclear SBUs into a 2D supermolecular layer. (f) The uninodal 4-connected **sql/Shubnikov** tetragonal plane net with $\{4^4 \cdot 6^2\}$ topology in complex **3**. Cu, pink; N, blue; O, red; PMo_{12}, brown; C, gray.

Structural description of $[Cu_2(H_2tda)_2(H_2O)_4]_2 \cdot [Cu_2(tda)_2(H_2O)_4] \cdot [HPW_{12}O_{40}] \cdot 18H_2O$ (4).

Complex **4** crystallizes in the triclinic crystal system with the $P\bar{1}$ space group. X-ray structure determination reveals that complex **4** is a 1D chain structure surrounded by di-nuclear Cu(II) clusters. The unit comprising six Cu(II) ions, four H_2tda ligands, two tda ligands, one $[PW_{12}O_{40}]^{3-}$ cluster (abbreviated to PW_{12}) and twenty water molecules (Figure 4a). Each PW_{12} cluster acts as a di-dentate inorganic ligand coordinating with two Cu(II) ions (Figure 4b). In **4**, there are three unique Cu(II) ions, the coordination environments of Cu1(II) and Cu2(II) are chemically equivalent, achieved by two nitrogen atoms from two tda ligands, and three oxygen atoms from one tda ligand and two water molecules. Cu3(II) is coordinated by two nitrogen atoms from two H_2tda ligands, and four oxygen atoms from one H_2tda ligand, one PW_{12} cluster and two water molecules. As a result, PW_{12} cluster are linked by Cu3(II) di-nuclear SBUs to form a 1D chain. While, the Cu1(II)-Cu2(II) di-nuclear SBUs are distributed around the 1D chains (Figure 4c).

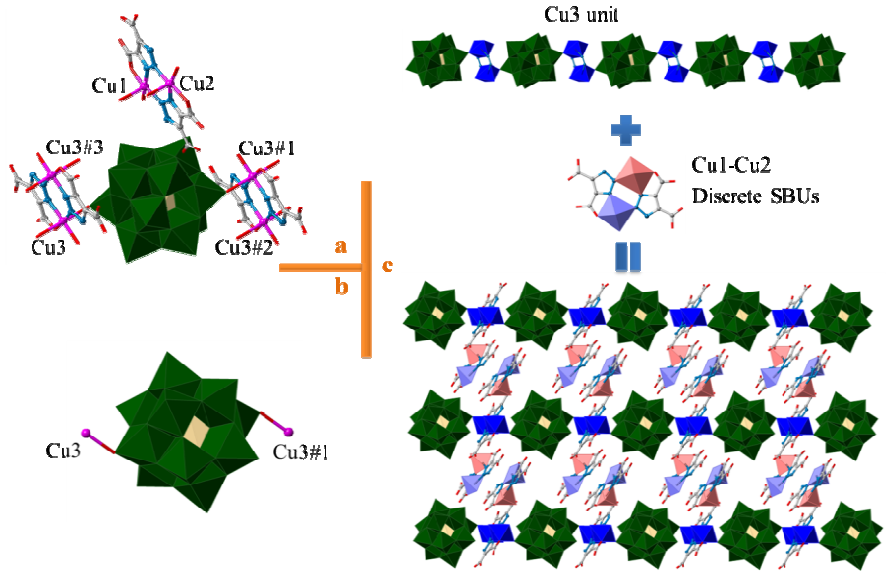

Figure 4. (a) Combined polyhedral and ball/stick representations of the molecular structure unit of **4**. All solvent molecules are omitted for clarity. (b) The coordination view of the PW_{12} cluster. (c) 1D chains surrounded by discrete SBUs. (symmetry code: #1: *-x, 1-y, 1-z*; #2: *x, -1+y, z*; #3: *-x, 2-y, 1-z*;).

Structural description of $[Cu_2(H_2tda)_2(H_2O)_4]\cdot[SiW_{12}O_{40}]\cdot(TMA)_2\cdot 3H_2O$ (5). Complex **5** crystallizes in the monoclinic crystal system with the *C*2/*c* space group. X-ray structure determination reveals that complex **5** is a 1D chain structure surrounded by TMA counterions. The structural unit comprises two Cu(II) ions, two H_2tda ligands, two TMA counterions, one $[SiW_{12}O_{40}]^{4-}$ cluster and seven water molecules (Figure 5a). Each SiW_{12} cluster acts as a di-dentate inorganic ligand coordinating with two Cu(II) ions (Figure 5b). In **5**, there is one unique Cu(II) ions, the Cu1(II) is coordinated by two nitrogen atoms from two H_2tda ligands, and four oxygen atoms from one H_2tda ligand, one SiW_{12} cluster and two water molecules. As a result, SiW_{12} cluster are linked by Cu1(II) di-nuclear SBUs to form a 1D chain. While, the TMA counter ions are distributed around the 1D chains (Figure 5c).

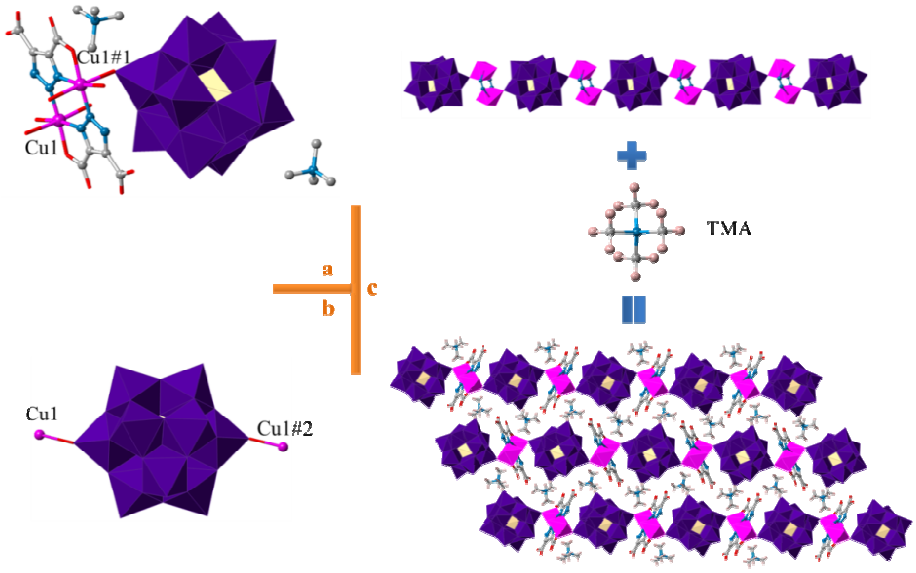

Figure 5. (a) Combined polyhedral and ball/stick representations of the molecular structure unit of **5**. All solvent molecules are omitted for clarity. (b) The coordination view of the SiW_{12} cluster. (c) 1D chains surrounded by TMA counter ion. (symmetry code: #1: 1.5-*x, -0.5-y, -z*; #2: 1.5-*x, -1.5-y, -z*;).

Structural description of $[Cu(H_2tda)(H_2O)_3]\cdot[SiW_{12}O_{40}]\cdot(TMA)_2\cdot H_2O$ (6). Complex **6** crystallizes in the monoclinic crystal system with the $P2_1/c$ space group. X-ray structure determination reveals that complex **6** is a 0D structure constituted of POM cluster, di-nuclear Cu(II) SBUs and TMA counter ions. The unit comprises one Cu(II) ions, one H_2tda ligands, two TMA counterions, one $[SiW_{12}O_{40}]^{4-}$ cluster and four water molecules (Figure 6 left). In **6**, there is one unique Cu(II) ion, the Cu1(II) is coordinated by two nitrogen atoms from two H_2tda ligands, and four oxygen atoms from one H_2tda ligand and three water molecules. There is no bonding among the constituents, which lead to the final 0D supermolecular structure (Figure 6 right).

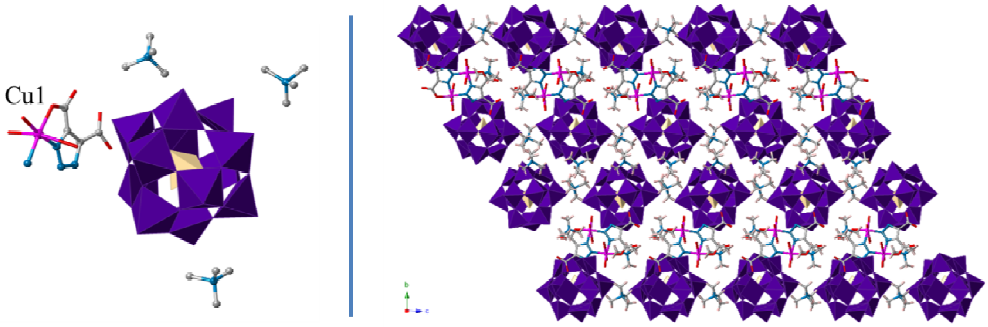

Figure 6. (left) Combined polyhedral and ball/stick representations of the molecular structure unit of **6**. All solvent molecules are omitted for clarity. (right) The stacking view of **6** along *c*

axis. (symmetry code: #1: 1-*x, -y,1-z*).

Influence of counterions, temperature and POM clusters on the structures of 1–6. The counter ions and temperature known to be the important factors in the modification of the structure of inorganic–organic hybrids. However, such an effect is seldom considered in the assembly of POM-based inorganic–organic hybrids, due to the difficulty in controlling the self-assembly processes. In this work, through changing the POM clusters, temperature and/or introducing counter ions, we have achieved the alternation of dimensionality to observe the effect of POM clusters, temperature and counter ions on the POM-based inorganic-organic hybrid assembly. First of all, we study the influence of the polyoxoanions on the structures of the complexes. As complexes **1** and **2** were synthesized under identical reaction conditions, except for alternation of the polyoxoanions (SiW_{12} for **1** and PMo_{12} for **2**), we deduce that the influence of the polyoxoanions on the final structures of **1** and **2** may arise from the differences in their valence. According to the matching charges, the $[SiW_{12}O_{40}]^{4-}$ polyoxoanions link four $[Cu(H_2tda)]^{+}$ units in **1**, while $[PMo_{12}O_{40}]^{3-}$ polyoxoanions link three $[Cu(H_2tda)]^{+}$ units in **2.** The high coordination numbers of $[SiW_{12}O_{40}]^{4-}$ polyoxoanions resulted in the complicated 3D structure for **1**. The relative lower coordination numbers of $[PMo_{12}O_{40}]^{3-}$ polyoxoanions lead to the 2D structure for **2**.

To investigate the influence of the temperature on the structures of the POM-based inorganic–organic hybrids, the reaction temperature of **2** is reduced from 100 ^{o}C to room temperature, and **3** were obtained. Although **2** and **3** display similar 2D structures, the 2D structure of **3** is extended *via* H-bonds. The possible reason for such a phenomenon is that the higher temperature conduct, the more covalent bonds are formed. Similar phenomenon is also observed in **5** and **6**.

To investigate the influence of the counterions on the structures of the POM-based inorganic–organic hybrids, the TMAH molecule is introduced into the reaction system of **1**, and **5** was obtained. As a result, the dimensionality framework of complex **5** is lower than that of **1**. Namely, the structure of **5** shows a 1D chain that SiW_{12} polyoxoanions connected by di-nuclear Cu(II) clusters. It is clear that the counter ion is a key factor in influencing the dimension of complex (3D for **1**, 1D for **5**). Because the TMAH counter ion couldn't participate in the coordination and hinder other building blocks to assemble. The system contain TMAH counterions all display the lower dimension: 1D for **4** and **5**, and 0D for **6**.

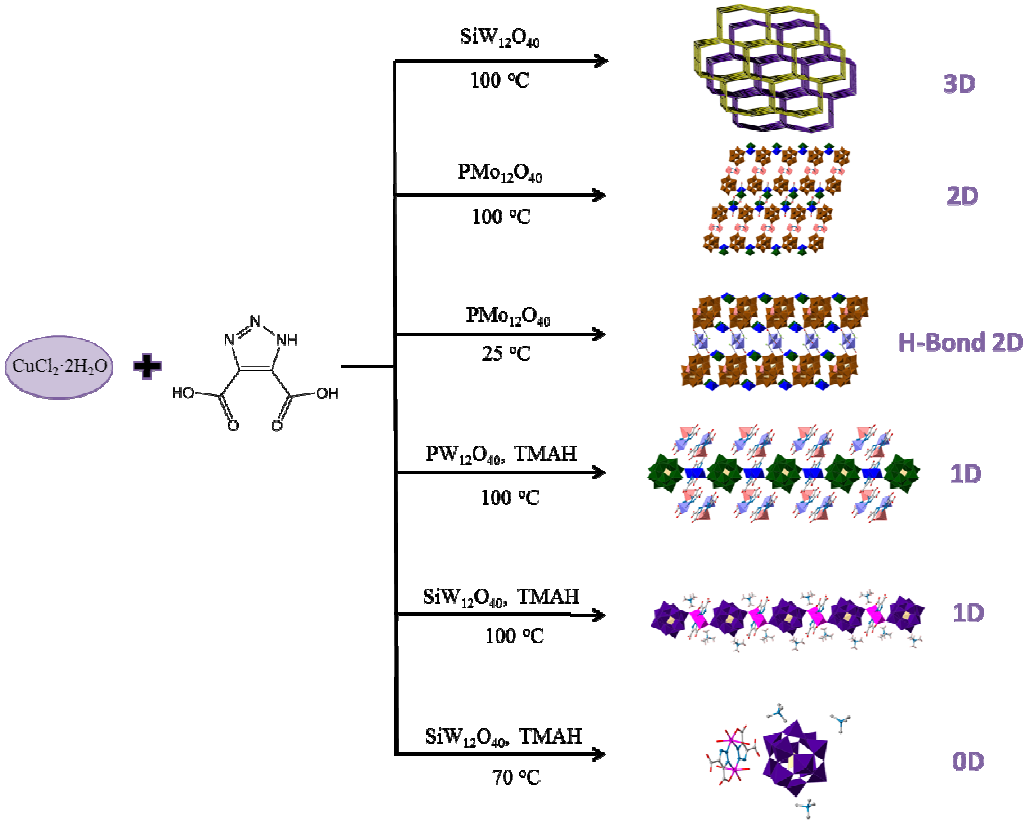

Scheme 1. Summary of the influences of the counterions, temperature and POM clusters on the structures of **1–6**.

Photocatalysis Properties

POMs have been studied as a green and cheap photocatalyst for the removal of organic pollutants or transition metal ions from water, due to the ultraviolet light induce POM to produce oxygen-to-metal charge transfer (OMCT) with promoting electron from the highest occupied molecular orbital (HOMO) to the lowest unoccupied molecular orbital (LUMO).[39] The charge transfer excited state (POM*) with strong oxidising properties can not only directly oxidize the target pollutant, but also react with water or other electron donors to generate an ·OH radical.[40] Rhodamine B (RhB) is common organic dyes in waste water, therefore it were selected as model pollutants to investigate their degradation in the presence of **1**, **5** and **6** in this work. The photodecomposition of Rhodamine-B (RhB) was evaluated under UV light irradiation through a typical process: 50 mg of **1**, **5** and **6** are mixed together with 100 ml of a 1.0×10^{-5}mol L^{-1} RhB solution in a beaker by ultrasonic dispersion for 10 min, respectively. The mixture was stirred for 0.5 h until it reached the surface-adsorption equilibrium (C_0) on the particles of **1**, **5** and **6**, respectively. Then, the mixture was stirred continuously under ultraviolet (UV) irradiation from a 125 W high pressure Hg lamp. At 20,

40, 60, 90, 120, 180, 240, 300 and 360 min, 3 ml of the sample was taken from the beaker, followed by several centrifugations to remove catalysts and a clear solution was obtained for UV-vis analysis. The photodegradation of RhB assisted by $(NBu_4)_4[SiW_{12}O_{40}]$ is shown in Figure 7b. After 360 min of irradiation, the maximum absorption band of the solution gradually shifts from 554 to 503 nm. The gradual hypsochromic shifts are caused by the N-deethylation of RhB during irradiation, namely, *N*,*N*,*N*′-triethylrhodamine (TER, 539 nm) and *N*,*N*′-diethyl rhodamine (DER, 522 nm), *N*-Ethyl-rhodamine (MER, 510 nm), Rhodamine (503 nm) which has been confirmed by Watanabe and co-workers.[41] When complexes **1**, **5** and **6** are used, the absorption peak of the dye at around 554 nm undergoes a fairly large decrease, and the hypsochromic shifts of the absorption band are considerably insignificant (Figure 7c-e). It is presumed that the cleavage of the whole chromophore structure of RhB occurs preferentially over the surface of complexes **1**, **5** and **6**. By irradiating **1**, **5**, **6** and $(NBu_4)_4[SiW_{12}O_{40}]$ for 360 min, the photocatalytic decomposition rate, defined as $1\text{-}C/C_0$, is 90%, 68%, 48% and 54%, respectively (Figure 7f), which illustrates that the formation of a POM-based complex can improve the photocatalytic performance of POMs. The stability of the catalysts were investigated based on the PXRD data. In comparison to the PXRD patterns before and after the catalytic process, there are no obvious changes, suggesting that complexes **1**, **5** and **6** are stable in the photocatalytic reaction system (Figure S19–21).

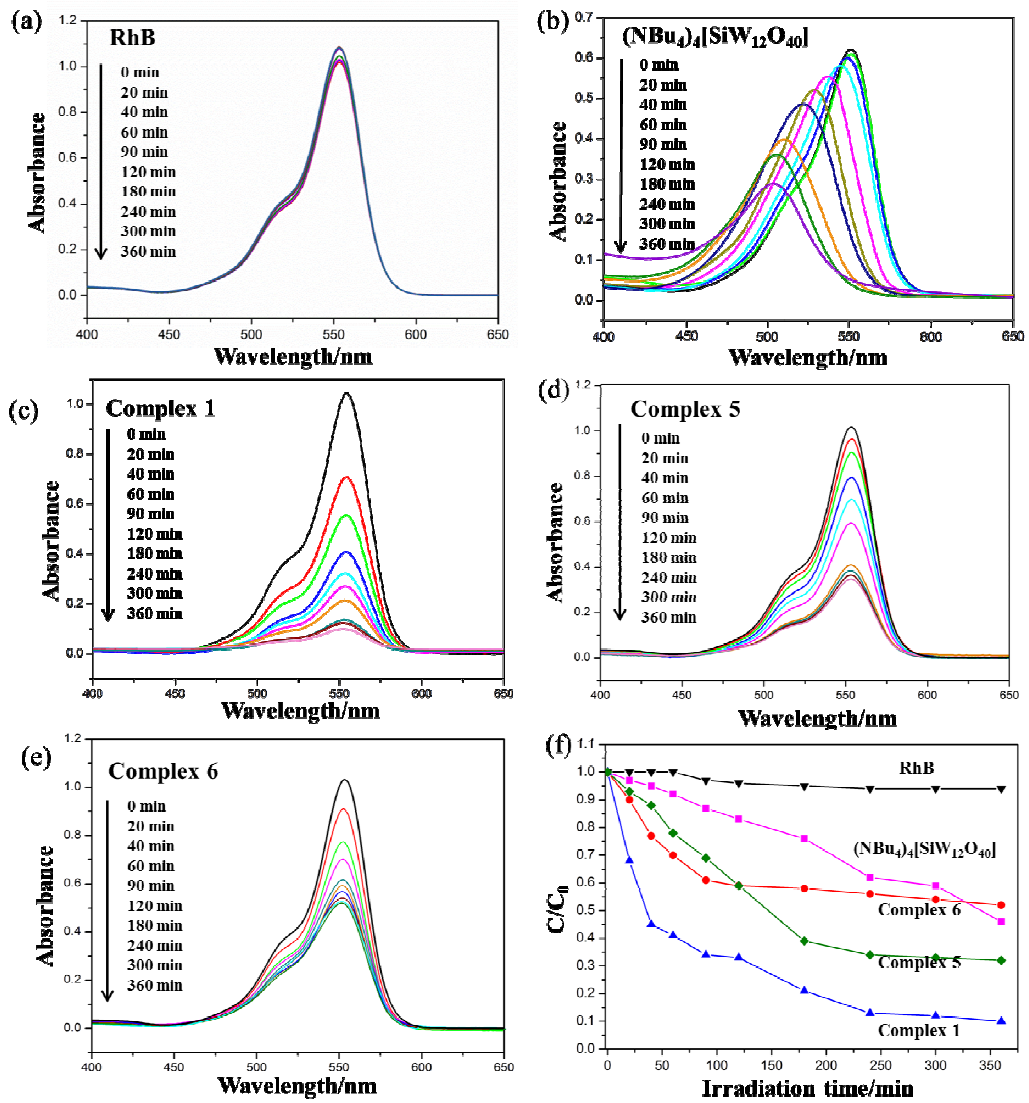

Figure 7. Absorption spectra of the RhB aqueous solution during the photodegradation under 125 W Hg-lamp irradiation with (a) no catalyst, (b) $(NBu_4)_4[SiW_{12}O_{40}]$ powder, (c) complex **1**, (d) complex **5**, (e) complex **6**, and (f) conversion rate of RhB with the reaction time.

CONCLUSIONS

Isolation of six new POM-MOF complexes with various dimensionalities and topologies demonstrates that the POM species, temperature and counterions dominate the structural variety of these POM-MOF complexes. E. g. the charges of POM polyoxoanions play a key role in controlling the coordination numbers of POMs; The high temperature facilitate to form high dimensionalities by forming more covalent bonds; the counterions efficiently hinder building blocks to assembly, which lead to the formation of lower dimensionalities. This approach provides step by step understanding on the assembly processes in terms of the

influences of POM clusters, temperature and counterions.

ASSOCIATED CONTENT

Supporting Information

Crystallographic, IR, TGA, and PXRD data. The Supporting Information is available free of charge on the ACS Publications website.

AUTHOR INFORMATION

Corresponding Author

*E-mail: gmli_2000@163.com.

Notes

The authors declare no competing financial interest.

ACKNOWLEDGMENTS

This work is financially supported by the National Natural Science Foundation of China (No. 21471051, 51472076, 21271089 & 51473046).

REFERENCE

1 A. Dhakshinamoorthy, A. M. Asiri, H. Garcia, *Chem. Soc. Rev.*, 2015, **44**, 1922.

2 J. R. Long, O. M. Yaghi, *Chem. Soc. Rev.* , 2009, **38**, 1213.

3 P. Deria, Y. G. Chung, R. Q. Snurr, J. T. Hupp, O. K. Farha, *Chem. Sci.*, 2015, **6**, 5172.

4 C. Orellana-Tavra, E. F. Baxter, T. Tian, T. D. Bennett, N. K. H. Slater, A. K. Cheetham, D. Fairen-Jimenez, *Chem. Commun.*, 2015, **51**, 13878.

5 L. Chen, Q. H. Chen, M. Y. Wu, F. L. Jiang, M. C. Hong, *Acc. Chem. Res.*, 2015, **48**, 201.

6 J. C. Jiang, O. M. Yaghi, *Chem. Rev.*, 2015, **115**, 6966.

7 N. W. Ockwig, O. Delgado-Friedrichs, M. O'Keeffe, O. M. Yaghi, *Acc. Chem. Res*., 2005, **38**, 176.

8 (a) A. U. Czaja, N. Trukhan, U. Muller, *Chem. Soc. Rev*., 2009, **38**, 1284; (b) S. T. Zheng, J. Zhang, G. Y. Yang, *Angew. Chem., Int. Ed*., 2008, **47**, 3909; (c) C. Abney, W. Lin, *Chem. Soc. Rev*., 2009, **38**, 1248; (d) G. Férey, *Chem. Soc. Rev*., 2008, **37**, 191; (e) M.

Eddaoudi, J. Kim, N. Rosi, D. Vodak, J. Wachter, M. O'Keeffe, O. M. Yaghi, *Science*, 2002, **295**, 469; (f) L. J. Murray, M. Dinca, J. R. Long, *Chem. Soc. Rev*., 2009, **38**, 1294.

9 X. Q. Du, Y. Ding, F. Y. Song, B. C. Ma, J. W. Zhao, J. Song, *Chem. Commun.*, 2015, **51**, 13925.

10 F. Bentaleb, O. Makrygenni, D. Brouri, C. C. Diogo, A. Mehdi, A. Proust, F. Launay, R. Villanneau, *Inorg. Chem.*, 2015, **54**, 7607.

11 J.-S. Qin, D.-Y. Du, W. Guan, X.-J. Bo, Y.-F. Li, L.-P. Guo, Z.-M. Su, Y.-Y. Wang, Y.-Q. Lan, H.-C. Zhou, *J. Am. Chem. Soc.*, 2015, **137**, 7169.

12 I. V. Kozhevnikov, *Catalysts for Fine Chemical Synthesis: Catalysis by Polyoxometalates*; Wiley: Chichester, U. K., 2002.

13 N. Mizuno, K. Kamata, S. Uchida, K. Yamaguchi, *In Modern Heterogeneous Oxidation Catalysis*; Mizuno, N., Ed.; Wiley-VCH: Weinheim, Germany, 2009.

14 J. M. Clemente-Juan, E. Coronado, A. Gaita-Arino, *Chem. Soc. Rev*., 2012, **41**, 7464.

15 L. B. Fullmer, R. H. Mansergh, L. N. Zakharov, D. A. Keszler, M. Nyman, *Cryst. Growth Des.*, 2015, **15**, 3885.

16 S. Wang, H. L. Li, D. Li, T. Y. Xu, S. L. Zhang, X. Y. Dou, L. X. Wu, *ACS Macro Lett.*, 2015, **4**, 974.

17 S. M. Lauinger, J. M. Sumliner, Q. S. Yin, Z. H. Xu, G. J. Liang, E. N. Glass, T. Q. Lian, C. L. Hill, *Chem. Mater*., 2015, **27**, 5886.

18 A. X. Tian, J. Ying, J. Peng, J. Q. Sha, Z. G. Han, J. F. Ma, Z. M. Su, N. H. Hu, H. Q. Jia, *Inorg. Chem*., 2008, **47**, 3274.

19 A. X. Tian, J. Ying, J. Peng, J. Q. Sha, H. J. Pang, P. P. Zhang, Y. Chen, M. Zhu, Z. M. Su, *Cryst. Growth Des*., 2008, **8**, 3717.

20 Z. Zhang, J. Yang, Y. Y. Liu, J. F. Ma, *CrystEngComm.*, 2013, **15**, 3843.

21 X. L. Wang, H. L. Hu, G. C. Liu, H. Y. Lin, A. X. Tian, *Chem. Commun*., 2010, **46**, 6485.

22 S. B. Li, H. Y. Ma, H. J. Pang, L. Zhang, *Cryst. Growth Des*., 2014, **14**, 4450.

23 X. L. Wang, N. Li, A. X. Tian, J. Ying, T. J. Li, X. L. Lin, J. Luan, Y. Yang, *Cryst. Growth Des*., 2014, **53**, 7118.

24 E. Burkholder, V. Golub, C. J. O'Connorr, J. Zubieta, *Inorg. Chem.*, 2004, **43**, 7014.

25 Y. Q. Lan, S. L. Li, K. Z. Shao, X. L. Wang, Z. M. Su, *Dalton Trans.*, 2008, 3824.

26 T. M. Anderson, W. A. Neiwert, K. I. Hardcastle, C. L. Hill, *Inorg. Chem.*, 2004, **43**, 7353.

27 C. Zhang, R. C. Howell, K. B. Scotland, F. G. Perez, L. Todaro, L. C. Francesconi, *Inorg. Chem*., 2004, **43**, 7691.

28 K. Suzuki, M. Shinoe, N. Mizuno, *Inorg. Chem*., 2012, **51**, 11574.

29 F. Yu, X. J. Kong, Y. Y. Zheng, Y. P. Ren, L. S. Long, R. B. Huang, L. S. Zheng, *Dalton Trans.*, 2009, 9503.

30 J. Y. Niu, J. A. Hua, X. Ma, J. P. Wang, *CrystEngComm*., 2012, **14**, 4060.

31 S. G. Mitchell, T. Boyd, H. N. Miras, D. L. Long, L. Cronin, *Inorg. Chem.*, 2011, **50**, 136.

32 R. Dessapt, D. Kervern, M. Bujoli-Doeuff, P. Deniard, M. Evain, S. Jobic, *Inorg. Chem*., 2010, **49**, 11309.

33 A. Leabani, R. Kawamoto, S. Uchida, N. Mizuno, *Inorg. Chem*., 2008, **47**, 3349.

34 More POM-MOFs examples see this reference cited. D. Y. Du, J. S. Qin, S. L. Li,; Z. M. Su, Y. Q. Lan, *Chem. Soc. Rev*., 2012, **41**, 7464.

35 J. Q. Sha, J. W. Sun, M. T. Li, C. Wang, G. M. Li, P. F. Yan, L. J. Sun, *Dalton Trans.*, 2013, 1667.

36 (a) J. P. Zhao, R. Zhao, W. C. Song, Q. Yang, F. C. Liu, X. H. Bu, *Cryst. Growth Des*., 2013, **13**, 437; (b) T. T. Zhao, X. M. Jing, J. Wang, D. M. Wang, G. H. Li, Q. S. Huo, Y. L. Liu, *Cryst. Growth Des.*, 2012, **12**, 5456; (c) D. Tian, S. J. Liu, Z. Chang, Y. H. Zhang, J. P. Zhao, X. H. Bu, *CrystEngComm*., 2013, **15**, 9344; (d) J. Y. Zou, H. L. Gao, W. Shi, J. Z. Cui, P. Cheng, *CrystEngComm*., 2013, **15**, 2682.

37 (a) G. M. Sheldrick, *Program for Structure Refinement*: University of Göttingen, Germany, 1997; (b) L. Farrugia, *J. Appl. Cryst*., 1999, **32,** 837; (c) G. M. Sheldrick, *SHELXL-97* (**1997**) Program for the Refinement of Crystal; (d) G. M. Sheldrick, *ActaCryst*., 1990, **A46**, 467; (e) G. M. Sheldrick, *ActaCryst*., 2008, **A64**, 112.

38 (a) T. L. Spek, *ActaCryst*., 1990, **A46**, c34; (b) J. Rohlicek, M. Husak, *J. Appl. Cryst*., 2007, **40**, 600.

39 (a) N. Mizuno and M. Misono, *Chem. Rev.*, 1998, **98**, 199; (b) S. Y. Gao, R. Cao, J. Lü, G. L. Li, Y. F. Li and H. X. Yang, *J. Mater. Chem.*, 2009, **19**, 4157; (c) S. Kim, J. Yeo and W. Choi, *Appl. Catal.*, *B*, 2008, **84**, 148.

40 S. Kim, H. Park andW.Choi, *J. Phys. Chem. B*, 2004, **108**, 6402.

41 (a) T. Watanabe, T. Takizawa, K. Honda, *J. Phys. Chem.*, 1977, **81**, 1845; (b) T. Takizawa, T. Watanabe, K. Honda, *J. Phys. Chem.*, 1978, **82**, 1391.

Graphic Abstract

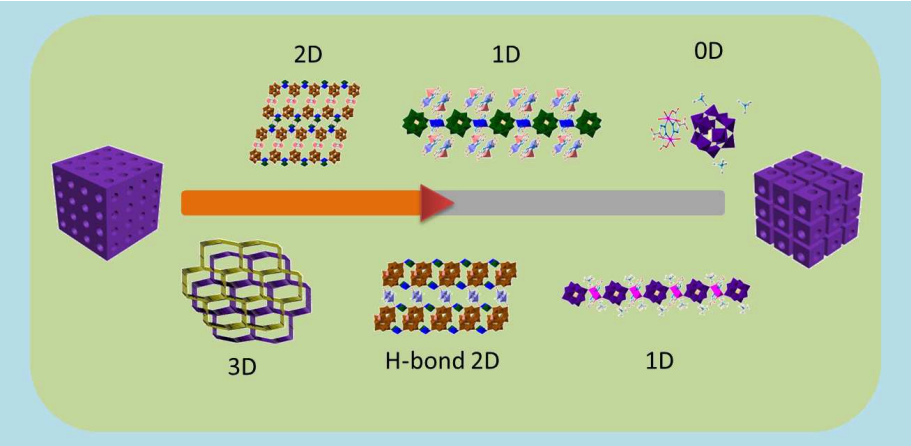

A series of six POM-based metal-organic frameworks with various dimensionalities have been isolated by tuning the reaction conditions (POM species, reaction temperature and counterions).